

# ERATO: event generator for four-fermion production at LEP2 energies and beyond

Costas G. Papadopoulos\*

Institute of Nuclear Physics, NRCPS Δημόκριτος, 15310 Athens, Greece

## ABSTRACT

ERATO is a Monte Carlo event generator describing four fermion production at LEP2 and beyond. All tree-order processes leading to four fermions are included, taking into account all relevant QCD contributions. QED higher order corrections are introduced via a structure function approach, whereas weak corrections related to fermion loops are also included. Special attention has been paid in studying the trilinear gauge couplings, and all possible contributions, including the CP-violating ones, have been implemented.

---

\* E-mail: Costas.Papadopoulos@cern.ch

## PROGRAM SUMMARY

*Title of the program:* ERATO. The name originates from  $\mathcal{E}\rho\alpha\tau\acute{\omega}$ , the ancient Greek Muse of lyric poetry.

*Program obtainable from:* Dr. Costas G. Papadopoulos, Institute of Nuclear Physics, NRCPS ‘Democritos’, 15310 Athens, Greece and using <ftp://alice.nrcps.ariadne-t.gr/pub/papadopo/erato>.

*Licensing provisions:* none

*Computer for which the program is designed and others on which it has been tested:* HP, IBM, ALPHA and SUN workstations.

*Operating system under which the program has been tested:* UNIX

*Programming language:* FORTRAN 77

*Keywords:* four-fermion processes, trilinear gauge couplings, event generator

*Nature of physical problem:* A very important fraction of the events produced at high-energy  $e^+e^-$  collisions corresponds to four-fermion final states. Important physical issues, like the measurement of the mass of the  $W$  boson and the study of the trilinear gauge couplings (TGC), are based on the analysis of these four-fermion final states. Other production processes, like associated Higgs production or R-parity violating SUSY particle production, lead also to the same final states. It is therefore indispensable to have a rather accurate description of the four-fermion production, including tree-order signal and background contributions as well as the leading part of the higher order corrections.

*Method of solution:* The construction of an event generator is of course the desired solution to the problem of calculating all four-fermion processes at high energies. To this end, we have calculated all relevant matrix elements, using a variation of the spinor technique which is more efficient in writing and testing the corresponding FORTRAN codes. A multichannel approach on phase space generation has been used in order to deal with the problem of the multipeak structure of the integrated function. Higher order corrections are systematically introduced and the new physics effects described effectively by the trilinear gauge couplings are considered. ERATO provides the computational framework which enables us to study in a systematic way four-fermion physics at high-energy  $e^+e^-$  colliders.

# LONG WRITE-UP

## 1 Introduction

LEP2 is already functioning at the highest energy ever reached for  $e^+e^-$  colliders. Moreover, machines capable to produce even higher energies, up to the TeV scale, like a Next Linear Collider (NLC), are nowadays thoroughly studied [1]. Most of the physicists working in the field think that new physics is to be expected at these energies and a lot of work has been done more than two decades now trying to develop theoretical frameworks to incorporate the expected ‘new phenomena’. On the other hand our current understanding of the elementary particle interactions, the so called Standard Model, is not yet completely tested due to the undetected Higgs particle a very important ingredient of the present theoretical apparatus. Any new dynamics in the Higgs sector of the theory will have very important consequences on the interactions among the heavy vector bosons,  $W$  and  $Z$  [2, 3]. In order to study these consequences, an accurate knowledge of the heavy vector boson production at these energies is indispensable and since heavy vector bosons always decay into light fermions, the four-fermion production is undoubtedly the first most interesting channel(s) to be studied at these energies. On the other hand, four-fermion will be a background channel for most of the interesting expected ‘new phenomena’, like SUSY particle production, new heavy vector boson contributions, etc.

ERATO is an event generator, which enables one to have an accurate description of the four-fermion dynamics. In this paper we will try to give a presentation of this program, starting with the main theoretical features and ending with a short description of how it works with a few illustrative examples. In section 2 a brief presentation of the amplitude and phase space calculations is given, in section 3 the main features of the FORTRAN code are described and finally in section 4 certain calculations are presented.

## 2 Computational Framework

### 2.1 Helicity Amplitudes

The first important step in order to construct an event generator is of course the calculation of all relevant tree-order matrix elements contributing to the processes under consideration. Our first approximation consists of neglecting the fermion masses, for all external fermion legs: this is of course a rather good approximation, since these terms are of the order of  $m_f^2/s$ , where  $m_f$  is the mass of the light fermion and  $s$  is the square of the center of mass energy. Nevertheless, this reasoning fails in the case of small angle scattering, a rather special case for which an approximation will be described in the sequel. In ERATO we have used a special representation of the so called ‘spinorial structure’ of the amplitudes, which follows more closely the structure of the Feynman graph under consideration, thus facilitating the writing and testing of the code. More specifically we are using the so called E-vector formalism[4, 5], which is based on the

following representation of the fermion ‘current’, for massless fermions:

$$E_\lambda^\mu(p_1, p_2) \equiv \bar{u}_\lambda(p_1) \gamma^\mu u_\lambda(p_2) \quad (1)$$

where

$$\begin{aligned} E_-^0 &= \sqrt{p_1^+ p_2^+} + \frac{(p_{1x} + ip_{1y})(p_{2x} - ip_{2y})}{\sqrt{p_1^+ p_2^+}} \\ E_-^x &= \sqrt{\frac{p_2^+}{p_1^+}}(p_{1x} + ip_{1y}) + \sqrt{\frac{p_1^+}{p_2^+}}(p_{2x} - ip_{2y}) \\ E_-^y &= -i \left( \sqrt{\frac{p_2^+}{p_1^+}}(p_{1x} + ip_{1y}) - \sqrt{\frac{p_1^+}{p_2^+}}(p_{2x} - ip_{2y}) \right) \\ E_-^z &= \sqrt{p_1^+ p_2^+} - \frac{(p_{1x} + ip_{1y})(p_{2x} - ip_{2y})}{\sqrt{p_1^+ p_2^+}} \end{aligned} \quad (2)$$

with  $p^\pm = p^0 \pm p^3$ .

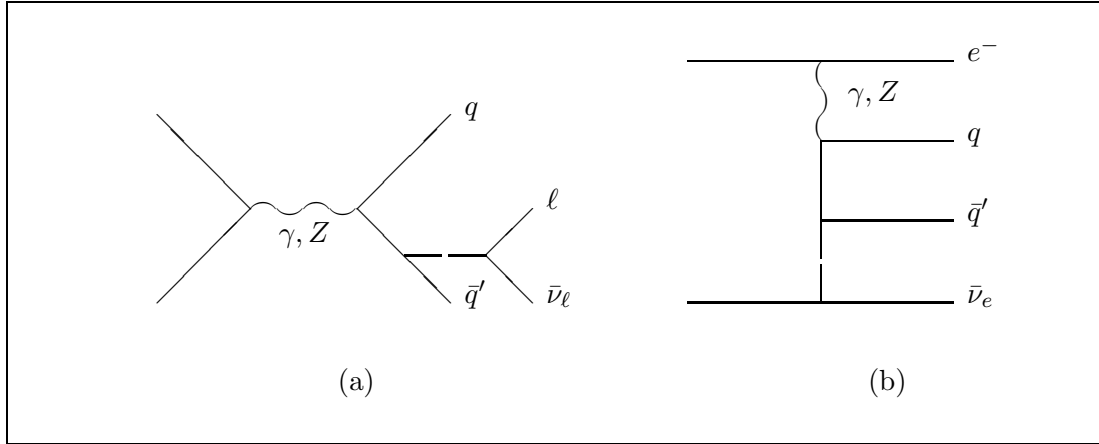


Figure 1: Feynman graphs contributing to  $e^+e^- \rightarrow e^-\bar{\nu}_e qq'$ .

Let us see how the Feynman graph of Fig.1(a), contributing to the process  $e^-(p_1)e^+(p_2) \rightarrow \ell(p_3)\bar{\nu}_\ell(p_4)q(p_5)\bar{q}'(p_6)$ , is computed in this formulation. First of all the spinorial part is simply written as:

$$\begin{aligned} &\bar{u}_-(p_5) \gamma^\mu (-\not{p}_6 - \not{p}_3 - \not{p}_4) \gamma^\nu u_-(p_6) \bar{u}_-(p_3) \gamma_\nu u_-(p_4) \bar{u}_\lambda(p_2) \gamma_\mu u_\lambda(p_1) \\ &= - \sum_{i=3,4,6} b_i E_-(p_5, p_i) \cdot E_-(p_3, p_4) E_-(p_i, p_6) \cdot E_\lambda(p_2, p_1) \end{aligned} \quad (3)$$

where  $b_i = \pm 1$  depending on whether the particle is outgoing or incoming and  $\lambda = \pm$  corresponds to the helicity of the incoming electron. Then coupling constants and propagators are combined to give the final expression. The graph of Fig.1(b) is simply computed by the interchange of  $p_2 \leftrightarrow p_3$  and  $b_2 \leftrightarrow b_3$ . All graphs have been computed using the above framework. Moreover where graphs involving as external particles massless bosons, as in the case of  $e^-e^+ \rightarrow q\bar{q}gg$

which contributes to the four-jet production channel and is experimentally indistinguishable from four-quark production, the polarization vector of the outgoing gluon is given by:

$$\epsilon^\mu(p; \lambda) \equiv \frac{1}{2\sqrt{p \cdot q}} E_\lambda^\mu(p, q) \quad (4)$$

The auxiliary four-vector  $q^\mu$  reflects the existence of the gauge invariance, always accompanying massless spin-1 particles, and provides a very powerful test of the computation, since any choice of  $q$  ( $q \cdot p \neq 0$ ) should give *exactly* the same result. Further details on the computation of the relevant color matrix can be found in references [6, 7].

## 2.2 Phase Space Generation

The next important part is of course the phase space generation. This follows closely the reasoning of references [8, 9]. The problem is that the amplitude we have to integrate over is a very complicated function of the kinematical variables, peaking at different regions of phase space. The idea is to define different kinematical mappings, corresponding to different peaking structures of the amplitude and then use an optimization procedure to adjust the percentage of the generated phase-space points, according to any specific mapping, in such a way that the total error is minimized. Let us present a very simple example in order to clarify these issues. The differential cross section is written as:

$$d\sigma = \frac{1}{2s} |\mathcal{M}|^2 d\text{Lips}(P; p_1, \dots, p_4) \quad (5)$$

where

$$d\text{Lips}(P; p_1, \dots, p_n) = (2\pi)^{4-3n} \prod_{i=1}^n \left( d^4 p_i \delta(p_i^2) \theta(p_i^0) \right) \delta\left(P - \sum_{i=1}^n p_i\right). \quad (6)$$

For the double resonant graph of Fig.2 and in order to describe efficiently its peaking structure we have naturally chosen the variables  $s_+ \equiv p_+^2 = (p_q + p_{\bar{q}'} )^2$  and  $s_- \equiv p_-^2 = (p_\ell + p_{\bar{\nu}_\ell})^2$  and write the invariant phase space as

$$d\text{Lips}(P; p_\ell, p_{\bar{\nu}_\ell}, p_q, p_{\bar{q}'}) = d\text{Lips}(P; p_+, p_-) \frac{ds_+}{2\pi} d\text{Lips}(p_+; p_q, p_{\bar{q}'}) \frac{ds_-}{2\pi} d\text{Lips}(p_-; p_\ell, p_{\bar{\nu}_\ell}). \quad (7)$$

In this way we have now the freedom to generate the integration variables  $s_\pm$  such that their distribution follows the well known Breit-Wigner form, namely

$$\frac{1}{(s_\pm - m_W^2)^2 + m_W^2 \Gamma_W^2}.$$

This is actually achieved in ERATO by the following mapping:

$$\begin{aligned} m_{q, \bar{q}'}^2 &= m_W^2 + m_W \Gamma_W \tan(\rho_1(y_+ - y_-) + y_-) \\ y_+ &= \tan^{-1}\left(\frac{E^2 - m_W^2}{m_W \Gamma_W}\right) \\ y_- &= \tan^{-1}\left(-\frac{m_W}{\Gamma_W}\right) \\ m_{\ell, \bar{\nu}_\ell}^2 &= m_W^2 + m_W \Gamma_W \tan(\rho_2(y'_+ - y_-) + y_-) \end{aligned}$$

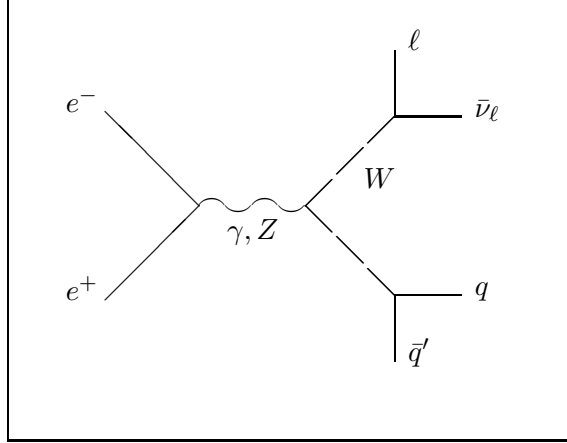


Figure 2: Double resonant graph contributing to  $e^+e^- \rightarrow \ell\bar{\nu}_\ell q\bar{q}'$ .

$$\begin{aligned}
y'_+ &= \tan^{-1}\left(\frac{(E - m_{q,\bar{q}'})^2 - m_W^2}{m_W\Gamma_W}\right) \\
\cos\theta_W &= 2\rho_3 - 1, \quad \phi_W = 2\pi\rho_4 \\
\cos\theta_\ell^* &= 2\rho_5 - 1, \quad \phi_\ell^* = 2\pi\rho_6 \quad (\text{in the } \ell, \bar{\nu}_\ell \text{ rest frame}) \\
\cos\theta_q^* &= 2\rho_7 - 1, \quad \phi_q^* = 2\pi\rho_8 \quad (\text{in the } q, \bar{q}' \text{ rest frame})
\end{aligned} \tag{8}$$

where  $\rho_i$ ,  $i = 1, \dots, 8$ , represent uniformly distributed pseudorandom numbers in  $(0,1)$ . In order to have a rather complete description of the process  $e^+e^- \rightarrow e^-\bar{\nu}_e q\bar{q}'$ , for example, sixteen different mappings have to be used. The number of mappings used is specific to each process and is appropriately defined in ERATO.

The large number of mappings, whose phase-space densities are described by the probability distributions  $g_i(\Omega)$ , naturally introduces the following representation of the total phase-space density:

$$g(\Omega) = \sum_i \alpha_i g_i(\Omega) \tag{9}$$

where  $\Omega$  stands for the phase space element and

$$\int d\Omega g(\Omega) = \int d\Omega g_i(\Omega) = \sum_i \alpha_i = 1. \tag{10}$$

The variables  $\alpha_i$ , are known as the *a priori weights*. Their main property is that the result of the MC integration is independent of them:

$$\int d\Omega f(\Omega) = \langle w \rangle \equiv \lim_{N \rightarrow \infty} \frac{1}{N} \sum_{i=1}^N \frac{f(\Omega_i)}{g(\Omega_i)}. \tag{11}$$

On the other hand the MC error depends on  $\alpha_i$ : this enables us to perform a *weight optimization* which could increase the speed of the MC integration<sup>1</sup>. This is achieved by minimizing the

<sup>1</sup>A detailed description can be found in reference [9].

variance estimator,  $W(\alpha) = \langle w^2 \rangle$ , with respect to  $\alpha_i$ , under the constraint  $\sum_i \alpha_i = 1$ . The optimization therefore is equivalent to the evaluation of the parameter values  $\alpha_i^{opt}$ , for which the MC error is minimized. This leads to the following set of equations:

$$W_i(\alpha) = W_j(\alpha), \text{ for all } i, j = 1, \dots, N$$

where

$$W_i(\alpha) = \left\langle \frac{g_i(\Omega)}{g(\Omega)} w^2 \right\rangle$$

with the MC weight  $w$  defined by

$$w = \frac{1}{g(\Omega)} \frac{1}{2s} |\mathcal{M}|^2.$$

ERATO uses an iterative algorithm to solve the above equations. The convergence of this procedure is checked by the evaluation of the variable

$$\mathcal{D} = \max_{i,j} |W_i - W_j| \quad (12)$$

which should vanish at the optimum point. In the numerical procedure  $\mathcal{D}$  measures indeed how well our  $\alpha$ 's approximate the optimum solution  $\alpha_i^{opt}$ .

### 2.3 Higher Order Corrections

A substantial part of the higher order corrections to the tree-level amplitudes have been taken into account in ERATO. As is well known the main part of these corrections comes from the emission of soft photons from the initial colliding particles. Although for neutral current processes, this ISR correction is a well defined, gauge-invariant quantity, for charged currents only the leading logarithmic (LL) part can be computed unambiguously. Nevertheless, this LL part accounts for most of these corrections, and therefore still it can be used to evaluate the ISR effect. In ERATO we have implemented the ISR in the structure function approach. This simply means that the true differential cross section is not given by Eq.(5), but by:

$$d\sigma_{\text{ISR}} = dx_1 dx_2 f(x_1) f(x_2) d\sigma(x_1 x_2 s) \quad (13)$$

where the momenta of the initial particles are given by,  $p_{e^-} = x_1 \frac{\sqrt{s}}{2} (1; 0, 0, 1)$  and  $p_{e^+} = x_2 \frac{\sqrt{s}}{2} (1; 0, 0, -1)$ . The explicit form of the function  $f(x)$  [10] is:

$$\begin{aligned} f(x) &= \frac{\exp\left(\left(-\gamma_E + \frac{3}{4}\right)\beta\right)}{\Gamma(1+\beta)} \beta (1-x)^{\beta-1} \\ &- \frac{1}{2}\beta(1+x) - \frac{1}{8}\beta^2 \left[ \frac{1+3x^2}{1-x} \log(x) + 4(1+x) \log(1-x) + 5+x \right] \end{aligned} \quad (14)$$

where  $\gamma_E$  is the Euler constant and

$$\beta = \frac{\alpha}{\pi} \left( \ln \frac{s}{m_e^2} - 1 \right),$$

with  $\alpha$  being the electromagnetic coupling constant.

An other important part of the higher order corrections is the so-called Coulomb correction. This is rather important at the threshold region,  $\sqrt{s} \sim 161$  GeV, reaching the level of 5%. It is the result of the long-range character of the electromagnetic interactions, contributing a factor roughly proportional to  $\alpha/\beta$ , which near threshold gives a substantial contribution. Its explicit form is

$$\sigma_{\text{Coul}} = \sigma_{\text{Born}}^{\text{CC3}} \frac{\alpha\pi}{2\bar{\beta}} \left[ 1 - \frac{2}{\pi} \arctan \left( \frac{|\beta_M + \Delta|^2 - \bar{\beta}^2}{2\bar{\beta} \text{Im}(\beta_M)} \right) \right], \quad (15)$$

with

$$\begin{aligned} \bar{\beta} &= \frac{1}{s} \sqrt{s^2 - 2s(p_+^2 p_-^2) + (p_+^2 - p_-^2)^2} \\ \beta_M &= \sqrt{1 - 4M^2/s}, \quad M^2 = m_W^2 - im_W \Gamma_W - i\epsilon \\ \Delta &= \frac{|p_+^2 - p_-^2|}{s}, \end{aligned} \quad (16)$$

and  $-\pi/2 < \arctan y < \pi/2$ . Here  $\bar{\beta}$  is the average velocity of the  $W$  bosons in their centre-of-mass system and CC3 refers to the three, double resonant graphs contributing to the on-shell  $W$  pair production,  $e^- e^+ \rightarrow W^- W^+$ .

Finally an important part of the radiative corrections is related to the width of the unstable particles,  $W$  and  $Z$  bosons. As it has been shown in references [5, 11] the corresponding corrections, which consist of resumming all closed fermionic-loop contributions to the two and three point functions, although necessary to restore gauge invariance of the calculation, is rather small at LEP2 energies, with the exception of final state topologies where an outgoing electron (or positron) is very close, essential parallel to the beam axis.

In order to describe the small angle scattering of processes with an  $e^-$  or  $e^+$  in the final state we have to take into account the small electron mass,  $m_e$ , leading to a further complication of the computational procedure. Nevertheless a very good estimate of the total massive cross section can be obtained by a rather simple approximation. This is achieved, at the leading logarithmic level[8], by introducing a cut on the angle of the outgoing, *massless* electron (or positron) given by:

$$\theta_m = \frac{m_e (p^0 - q^0)}{p^0 q^0}, \quad (17)$$

where  $p^0$  ( $q^0$ ) is the energy of the incoming (outgoing) electron. In all cases we have checked, this approximation gives a rather good estimate of the total massive cross section.

We conclude this section by underlining the fact that ERATO has historically been designed for TGC studies and followed an older MC for single  $W$  production [4]. Moreover in the present version of ERATO, all TGC deviations, including CP violating ones, are considered<sup>2</sup>.

### 3 Program Structure

The complete file system is organized as follows:

---

<sup>2</sup> For a detailed presentation of TGC interactions, see reference[12]

flag IPRO	processes	type of graphs
1	$\nu_\mu \bar{\nu}_\mu \nu_\tau \bar{\nu}_\tau$	NC6
2	$\nu_\mu \bar{\nu}_\mu \nu_\mu \bar{\nu}_\mu$ $\nu_\tau \bar{\nu}_\tau \nu_\tau \bar{\nu}_\tau$	NC12
3	$\nu_\mu \bar{\nu}_\mu \tau^+ \tau^-$ $\nu_\tau \bar{\nu}_\tau \mu^+ \mu^-$	NC10
4	$\mu^+ \mu^- \tau^+ \tau^-$	NC24
5	$\mu^+ \mu^- \mu^+ \mu^-$ $\tau^+ \tau^- \tau^+ \tau^-$	NC48
6	$e^+ e^- \nu_\mu \bar{\nu}_\mu$ $e^+ e^- \nu_\tau \bar{\nu}_\tau$	NC20
7	$e^+ e^- \mu^+ \mu^-$ $e^+ e^- \tau^+ \tau^-$	NC48
8	$e^+ e^- e^+ e^-$	NC144

Table 1: Physical processes in program llll\_n.

flag IPRO	processes	type of graphs
1	$\mu^+ \mu^- \nu_\mu \bar{\nu}_\mu$ $\tau^+ \tau^- \nu_\tau \bar{\nu}_\tau$	NC12+CC7
2	$e^+ e^- \nu_e \bar{\nu}_e$	NC24+CC14+CC18
3	$\mu^+ \mu^- \nu_e \bar{\nu}_e$ $\tau^+ \tau^- \nu_e \bar{\nu}_e$	NC12+CC9
4	$\nu_\mu \bar{\nu}_\mu \nu_e \bar{\nu}_e$ $\nu_\tau \bar{\nu}_\tau \nu_e \bar{\nu}_e$	NC6+CC6
5	$\nu_e \bar{\nu}_e \nu_e \bar{\nu}_e$	NC18+CC18

Table 2: Physical processes in program llll\_c1.

1. **ffiles** contains the seven FORTRAN files (**\*.f**) where the computation of the corresponding processes is performed. More specifically, tables 1-7 give the physical processes which can be obtained by each FORTRAN program. Also shown is the corresponding value of the flag IPRO which is used as an input. When more than one physical processes are assigned to a given value of the IPRO, it means that all these processes share identical description. Finally the number of Feynman graphs contributing to the current process is also presented. The nomenclature NC24, CC10, etc stands for Neutral or Charged Currents and is related to the unstable states contributing to a given process.
2. **inputs** contains the corresponding input files used in the actual version.
3. **demo** contains the corresponding Make file used for compilation and linking as well as a test run output.
4. **share** contains all commonly used subroutines and functions, such as the function **EVECTOR** and the pseudo-random number generator(s).

flag IPR0	processes	type of graphs
1	$\mu^- \bar{\nu}_\mu \tau^+ \nu_\tau$ $\mu^+ \nu_\mu \tau^- \bar{\nu}_\tau$	CC9
2	$e^- \bar{\nu}_e \mu^+ \nu_\mu$ $e^- \bar{\nu}_e \tau^+ \nu_\tau$ $e^+ \nu_e \mu^- \bar{\nu}_\mu$ $e^+ \nu_e \tau^- \bar{\nu}_\tau$	CC18

Table 3: Physical processes in program llll\_c2.

flag IPR0	processes	type of graphs
1	$\nu_\mu \bar{\nu}_\mu D \bar{D}$ $\nu_\tau \bar{\nu}_\tau D \bar{D}$	NC10
2	$\nu_\mu \bar{\nu}_\mu U \bar{U}$ $\nu_\tau \bar{\nu}_\tau U \bar{U}$	NC10
3	$\mu^+ \mu^- U \bar{U}$ $\tau^+ \tau^- U \bar{U}$	NC24
4	$\mu^+ \mu^- D \bar{D}$ $\tau^+ \tau^- D \bar{D}$	NC24
5	$e^+ e^- U \bar{U}$	NC48
6	$e^+ e^- D \bar{D}$	NC48

Table 4: Physical processes in program llqq.

The codes are very flexible and easily accessible to the user, so that any update can easily be implemented. It should be noted however that no special FORTRAN-optimization has been performed in the writing of the code. Nevertheless the time needed for event generation is rather small, so for all usual applications such an optimization is not really necessary.

Let us start with the main common variables used in the program. The first of course is P(1:4,1:20), where all particle momenta are stored: P(4,1:20) refers to the energy and P(1:3,1:20) to the three-momentum,  $p_x, p_y, p_z$ . At the beginning of each program (e.g. llll\_n.f), the momentum assignment of the final particles is explicitly given, e.g.  $\mu^-(p_3) \bar{\nu}_\mu(p_4) u(p_9) \bar{d}(p_{10})$ . Variable P(1:4,1) refers to the incoming electron and P(1:4,2) to the incoming positron. Included in the same common MOM is the array B(1:20) which as

flag IPR0	processes	type of graphs
1	$\nu_e \bar{\nu}_e U \bar{U}$	NC12+CC7
2	$\nu_e \bar{\nu}_e D \bar{D}$	NC12+CC7

Table 5: Physical processes in program neneqq.

flag IPRO	processes	type of graphs
1	$\mu^- \bar{\nu}_\mu U \bar{D}$ $\tau^- \bar{\nu}_\tau U \bar{D}$	CC10
2	$e^- \bar{\nu}_e U \bar{D}$	CC20
3	$\mu^+ \nu_\mu U \bar{D}$ $\tau^+ \nu_\tau U \bar{D}$	CC10
4	$e^+ \nu_e D \bar{U}$	CC20

Table 6: Physical processes in program evud.

flag IPRO	processes	type of graphs
1	$U \bar{U} D \bar{D}$	CC11+NC24+QCD8
2	$U \bar{U}' D' \bar{D}$	CC11
3	$U \bar{U} U \bar{U}$	NC48+QCD16
4	$D \bar{D} D \bar{D}$	NC48+QCD16
5	$U \bar{U} U' \bar{U}'$	NC24+QCD8
6	$U \bar{U} D' \bar{D}'$	NC24+QCD8
7	$D \bar{D} D' \bar{D}'$	NC24+QCD8
8	$U \bar{U} g g$ $D \bar{D} g g$	QCD8

Table 7: Physical processes in program qqqq.

explained in the previous section, takes the values  $\pm 1$  if the particle is outgoing (incoming). Physical constants are included in the common `PHYS`.

The main routine where the helicity amplitudes are calculated, is called `MASTER`. The array `WTI(1:2,1:NITER)` gives the amplitude squared, for  $\mp$  helicities of the incoming electron, whereas `NITER` refers to different input values for non-standard TGC, with `ITER=1` always returning the Standard Model value. `MASTER` is called by the routine `EVENT` after the phase-space point generation has been performed. This is done by first producing the appropriate energy fractions `X1` and `X2`, when `ISR` is on (flag `ISR=1`), which define the reduced c.m.s. energy,  $s = x_1 x_2 s_0$ . Notice that the generation of these variables follows the function `FISR(X)` which is the product of the corresponding structure functions given by Eq.(14). Then the routine `ADDRESS` is called, which returns the phase space point, according to the given phase-space mapping, labeled by the flag `IGEN`. The flag `IFLAG` is used as follows: when `IFLAG=0`, the phase space point is generated whereas for `IFLAG=1` the phase space density is computed. Of course, as explained in the previous section, the distribution among the different mappings is governed by the values of  $\alpha_i$ , `ALPHA(1:NGEN)`, where `NGEN` is the total number of mappings used in the actual calculation. Optimization on the values of  $\alpha_i$ , which means redefinition of them, is performed after certain iterations defined by the variable `IBASE`. `EVENT` is finally returning the value of

the variable `WTI(1:2,1:NITER)`, which corresponds to the MC weight of the given phase-space point (event). The driving routine is called `DRIVE`, which takes the weight coming from `EVENT` and then performing all relevant sums. A schematic representation of the flow of the program is given in Fig.3.

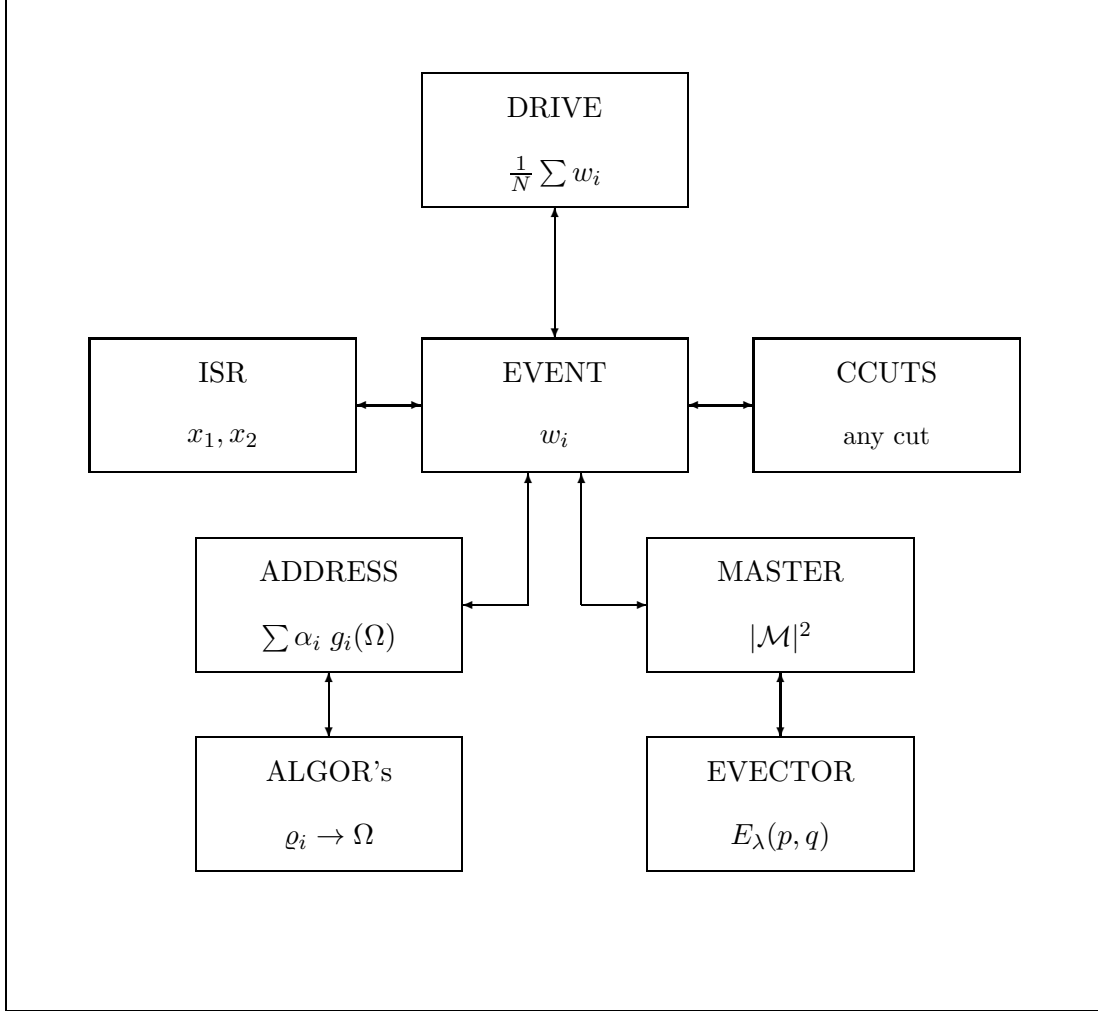


Figure 3: The flow-chart of the program.

For the cases where  $WW\gamma$  and  $WWZ$  vertices appear, as for example in the `evud.f` code, the flag `INAIVE` is used to distinguish between different ways of treating the width of the unstable particles. As explained in detail in reference [11], the fixed width solution, corresponding to the `INAIVE=1` can be safely used by default. `INAIVE=0` and `INAIVE=2` correspond to the ‘fudge-factor’ schemes [13], whereas `INAIVE=5` to the running width, without corrections to the  $WW\gamma$  and  $WWZ$  vertices, which of course at small momentum transfer gives inconsistent results. Finally `INAIVE=3` correspond to the inclusion of all the imaginary-parts of the fermion-loop corrections, in a way consistent with both  $U(1)$  and  $SU(2)$  gauge invariance.

In order to avoid singularities of the massless amplitude as well to be as close as possible to the experimental picture cuts are applied in the usual sense. In the present version we have implemented the so-called Canonical Cuts, used in the LEP2 workshop analyses. Of course any cut can be trivially implemented. In the case of ISR, there is an additional cut on the reduced energy of the  $e^+e^-$  system, defined by the variable SCUT.

All matrix elements have been tested against the MadGraph [14] calculations to sixteen digits accuracy. Also consistency checks related to  $U(1)$  and  $SU(2)$  gauge invariance, or equivalently to the *high-energy unitarity* have been performed. Finally ERATO has been participated to the comparisons tests made at the LEP2 workshop [15], where a very accurate check on the generator as a whole has been successfully performed.

## 4 Test Run

A typical input file is as follows:

```

1                *process
1                *iterations
1                *ISR
0                *ICOULOMB
128.07 0.2310309 91.1888 2.4974 80.23 2.033 *input parameters
0                *cuts(total xs)
1.0 1.0          *cmax(cmin) cmas
175             *energy
200000          *nev
2500            *IEV
1                *0 no optimization
1                *naive
1.0 2. 1.5 2.0 0.8 0.5 0.0
0.0 1. 0.5 1.0 -0.2 -0.5 -1.0
0.0 1. 0.5 1.0 -0.2 -0.5 -1.0
2                *icase

```

This is read by the `evud` program. The process under consideration is defined by the flag `IPRO`. The `NITER` corresponds to how many iterations the code will perform in order to calculate the weight for `NITER` different values of the TGC parameters (default=1). Then `ISR` defines the use of initial state radiation (on=1, off=0). The same for `ICOULOMB` which is the case of the Coulomb correction. The input parameters correspond to  $1/\alpha_{em}$ ,  $\sin^2 \theta_w$ ,  $m_Z$ ,  $\Gamma_Z$ ,  $m_W$ ,  $\Gamma_W$  respectively. The flag `ITOTAL`, in case it takes the value 1, will use the approximation described by Eq.(17) for computing an estimate of the total massive cross section. `CMAX(CMIN)` and `CMASS` are variables used by the generator algorithms and can be put to their limits, `CMAX=1` and `CMASS=0` respectively. Then the energy and the number of MC iterations (`NEV`) are given. Variable `IEV` defines the first time when optimization will take place and the flag `IOPT` switch on (off) this procedure. `INAIVE` governs the width scheme to be used, with `INAIVE=1` being the fixed width, and `INAIVE=5` the naive running width. Several other options are available for specific processes, which can be

found in the distributed codes. Then NITER values for TGC parameters with Standard Model values 1 and 0 respectively are read by the program (the remaining terms are not read). Finally the flag ICASE pick up the desired TGC parameter-relation scheme<sup>3</sup>, known as  $a_{B\Phi}$  (ICASE=0),  $a_{W\Phi}$  (ICASE=2) and  $a_W$  (ICASE=3) as well as other choices which can easily be found in the distributed subroutine MASTER.

The output, apart from monitoring printings, looks as follows:

```

ISR= 1
ICOULOMB= 1
STARTING AT-----Wed Jul 31 22:18:49 1996
THIS IS THE STARTING POINT
ITOTAL = 0
CMAX = 1.0  CMASS = .5
E= 175.0
NEV= 250000
1./ALPHA,ZLO,ZETA,GEUL,GAB
137.036 25.53137686693119 5.698195932780109E-02 .5772156649015319
.9701624225753434
EO,ELMAS,ZETA1,SCUT
175.0 5.000000000000000E-04 17.54941409170019 1.0
RM48 INITIALIZED:      0      0      0
CANONICAL CUTS 1.0 3.0 .984807753012208 .9961946980917455 25.0 1

ICASE= 2

IMPROVMENT FOUND
DISTANCE= 6.855963070506428E-06
EVENTS 2500.0 2500
IMPROVMENT FOUND
DISTANCE= 1.797322661221867E-06
EVENTS 7500.0 10000
IMPROVMENT FOUND
DISTANCE= 1.019962512017920E-06
EVENTS 10000.0 20000
IMPROVMENT FOUND
DISTANCE= 7.980700337882255E-07
EVENTS 20000.0 40000
IMPROVMENT FOUND
DISTANCE= 6.970462448481489E-07
EVENTS 40000.0 80000
IMPROVMENT FOUND
DISTANCE= 6.011073515995931E-07

```

---

<sup>3</sup>For a detailed analysis on these TGC parameters, see reference [16].

EVENTS 80000.0 160000

ALPHA( 1) = .000  
ALPHA( 2) = .298  
ALPHA( 3) = .006  
ALPHA( 4) = .003  
ALPHA( 5) = .003  
ALPHA( 6) = .006  
ALPHA( 7) = .683

ENERGY = 175.0000

ANOMALOUS MAG.MOMENT OF W=  
.00000E+00 1.0000 1.0000 .00000E+00 .00000E+00

SIGMA= .4875463E-03 +- .1390471E-05NB

SIGMA= .3478089E-05 +- .1243032E-07NB

TOTAL SIGMA ERROR  
.491024E-03 .138875E-05

ICASE= 2

[TOTAL,PASS,FAIL,ICUT] : 250000241945 8055 4789 1479 815 972

GENERATOR 784 78252 3938 3030 2968 4178 156850 0 0 0 0 0 0 0 0 0 0  
0

[MAXIMUM WT=] 1.489366913311956E-02

ENDING AT-----Wed Jul 31 23:56:49 1996

This is a run for the process  $e^-e^+ \rightarrow \mu^-\bar{\nu}_\mu u\bar{d}$ . The variables SIGMA give the left and right handed helicity contributions with respect to the initial electron. The TOTAL SIGMA and ERROR are the total cross section and its MC error. The flag IMPROVEMENT FOUND refers to the result of the optimization and the final values of  $\alpha_i$  are also printed out. The variable DISTANCE refer to  $\mathcal{D}$  as defined in Eq.(12). Finally the values of the canonical cuts,  $E_\ell$ ,  $E_{jet}$ ,  $\cos\theta_\ell$ ,  $\cos\theta_{(\ell,jet)}$  and  $m_{jet-jet}^2$  are presented after the flag CANONICAL CUTS. All the other elements in the output are more or less self-explanatory.

## Acknowledgements

I would like to thank the Department of Physics of the University of Durham, where a substantial part of this work has been done. It is also a pleasure to thank the DELPHI collaboration and especially, M. Gibbs, H. Phillips, R. Sekulin and S. Tzamarias for their helpful suggestions and support during the writing of the generator. I would like also to thank G. Daskalakis for proofreading the manuscript. This work was partially supported by the EU grant CHRX-CT93-0319.

## References

- [1] ‘ $e^+e^-$ : the physics potential’ by P.M. Zerwas, (ed.) (DESY). 1993. Hamburg, Germany: DESY (1993) 602 p, and Hamburg DESY - DESY 93-123 (93/12) 602 p.
- [2] K. Gaemers and G. Gounaris, Z.Phys. **C1**(1979) 259.
- [3] G.J. Gounaris and F.M. Renard, Z.Phys. **C59** (1993) 133.
- [4] E.N. Argyres and C.G. Papadopoulos, Phys. Lett. **B263** (1991) 298.
- [5] C.G. Papadopoulos, Phys. Lett. **B352** (1995) 144.
- [6] E. N. Argyres, C.G. Papadopoulos and S. D. P. Vlassopoulos, Phys. Lett. **B237** (1990) 581-587.
- [7] E. N. Argyres, O. Korakianitis, C.G. Papadopoulos and S. D. P. Vlassopoulos, Nucl. Phys. **B354** (1991) :1-23.
- [8] F.A. Berends R. Kleiss and R. Pittau, Nucl. Phys. **B424** (1994) 308 and Comp. Phys. Commun. **85** (1995) 437.
- [9] R.Kleiss and R.Pittau, Comp. Phys. Commun. **83** (1994) 141.
- [10] W. Beenakker *et al.*, ‘ $WW$  cross sections and distributions’ in *Physics at LEP2*, ed. G. Altarelli *et al.*, Vol.1, p. 79, CERN 96-01, February 1996 & hep-ph/9602351.
- [11] E.N. Argyres *et al*, Phys.Lett. **B358** (1995) 339
- [12] G. Gounaris *et al.*, ‘Triple gauge boson couplings’ in *Physics at LEP2*, ed. G. Altarelli *et al.*, Vol.1, p. 525, CERN 96-01, February 1996 & hep-ph/9601233.
- [13] U. Baur, J.A.M. Vermaseren and D. Zeppenfeld, Nucl. Phys. **B375** (1992) 3-44.
- [14] T. Stelzer and W.F. Long, Comp.Phys.Comm. **81** (1994) 357-371.
- [15] D. Bardin *et al.*, ‘Event generators for  $WW$  physics’ in *Physics at LEP2*, ed. G. Altarelli *et al.*, Vol.2, p. 3, CERN 96-01, February 1996.
- [16] Costas G. Papadopoulos, ‘*Studying trilinear gauge couplings at LEP2 using optimal observables*, May 1996, hep-ph/9605303, to appear in Physics Letters B.